Lab on a Chip

PAPER

View Article Online
View Journal | View Issue

Cite this: *Lab Chip*, 2018, **18**, 1928

A fully-integrated and automated testing device for PCR-free viral nucleic acid detection in whole blood†

Wenhan Liu,[a] Jagotamoy Das,[b] Adam H. Mepham,[a] Carine R. Nemr,[c] Edward H. Sargent[d] and Shana O. Kelley *[abce]

Received 9th April 2018,
Accepted 29th May 2018

DOI: 10.1039/c8lc00371h

rsc.li/loc

Integrated devices for automated nucleic acid testing (NAT) are critical for infectious disease diagnosis to be performed outside of centralized laboratories. The gold standard methods for NAT are enzymatic amplification methods like the polymerase chain reaction that typically require expensive equipment and highly-trained personnel, limiting use in low-resource settings. A low-cost, integrated, rapid, portable and user-friendly point-of-care (POC) nucleic acid diagnostic device will improve the accessibility of NAT. Here, we present a fully integrated and simple-to-use POC device operated by a passive fluidic method that is able to perform a sequential multi-step assay to detect viral nucleic acids in blood. This simple device enabled the rapid detection of hepatitis C virus in blood in approximately 30 minutes with minimal sample handling by the user.

Introduction

Nucleic acid testing (NAT) is used for a variety of applications such as genetic analysis, disease diagnosis, food safety, and environmental monitoring. Highly-sensitive and selective molecular diagnostic techniques for NAT that use the polymerase chain reaction (PCR) or other enzymatic amplification approaches have quickly become the gold standard for diagnosing infectious diseases. However, the use of PCR requires expensive equipment and highly trained personnel, which limit its use in lab-free settings. Recently, considerable effort has been directed towards making NAT accessible in resource-limited settings through the development of low-cost point-of-care (POC) diagnostic devices.[1–4]

The ideal integrated POC NAT device should be portable and provide affordable, rapid and automated detection with minimal user handling steps.[1,2,5,6] Such a device should also be able to handle complex biological fluids such as whole blood, which can be challenging to work with for molecular detection. A variety of POC NAT devices that could be used for molecular diagnostic testing have been developed. These devices typically employ paper or traditional microfluidics and measure changes in colour,[7–10] fluorescence,[5,11–15] electrical properties,[16] electrochemical signals[17–20] and magnetism[21] for sample analysis. Such devices are able to improve NAT accessibility by either eliminating the need for PCR amplification[16,20] or providing inexpensive on-chip amplification of targets.[5,7–15,17–19,21]

However, the POC NAT devices developed to date still have limitations for true sample-to-answer testing. Easy to fabricate devices[7,9,10,12,13,15] using economical materials are able to reduce the cost of detection but require the user to perform multiple manual sample processing, fluid manipulation or device handling steps during their operation. On the other hand, simple-to-use, fully integrated and automated devices[5,8,17] that offer user-friendly operation are often difficult and complex to fabricate and/or require large external accessories to operate. The majority of devices in both of these categories also require target amplification prior to detection, which can increase assay time. Although PCR-free devices that have been reported are promising alternatives for rapid molecular detection, those reported to date are still not able to integrate and automate the complex sample processing steps required for user-friendly, sample-to-answer molecular testing.

Here, we present a new device operated using passive fluidics that integrates the sample processing steps (plasma separation from whole blood and viral lysis) with electrochemical nucleic acid detection. The hepatitis C virus (HCV) was used to

[a] *Institute for Biomaterials and Biomedical Engineering, University of Toronto, Toronto, M5S 3G9 Canada. E-mail: shana.kelley@utoronto.ca*
[b] *Department of Pharmaceutical Science, Leslie Dan, Faculty of Pharmacy, University of Toronto, Toronto, M5S 3M2 Canada*
[c] *Department of Chemistry, Faculty of Arts and Science, University of Toronto, Toronto, M5S 3H4 Canada*
[d] *Department of Electrical and Computer Engineering, Faculty of Engineering, University of Toronto, Toronto, M5S 3G4 Canada*
[e] *Department of Biochemistry, Faculty of Medicine, University of Toronto, Toronto, M5S 1A8 Canada*

† Electronic supplementary information (ESI) available. See DOI: 10.1039/c8lc00371h

validate the integrated device. HCV diagnosis currently involves an antibody-based screening test followed by confirmation and genotyping based on NAT; this type of testing could significantly benefit from rapid and low-cost NAT detection in an integrated device to eliminate the existing two-step process. The device we describe is capable of detecting clinically-relevant concentrations of HCV in blood in approximately 30 minutes. Additionally, it is low cost, requires minimal sample preparation and handling, is portable, and allows for rapid target detection—fulfilling all of the desired properties of an ideal device for use at the POC. Furthermore, it serves to bridge the gap between POC devices that are inexpensive to fabricate but cumbersome to operate and those that are more expensive to fabricate but offer simple operation.

Materials and methods

Materials

Acetone, isopropyl alcohol (IPA), anhydrous ethanol, gold chloride ($HAuCl_4$), hydrochloric acid (HCl), palladium chloride ($PdCl_2$), perchloric acid ($HClO_4$), calcium oxide (CaO), 6-mercaptohexanol (MCH), tryptic soy broth (TSB), glycerol, Whatman cellulose chromatography papers 3MM Chr sheets, hexaammineruthenium(III) chloride ($Ru(NH_3)_6Cl_3$) and potassium ferricyanide ($K_3[Fe(CN)_6]$) were acquired from Sigma-Aldrich, MO. IPVH00010 Immobilon-P polyvinylidene fluoride (PVDF) membrane 0.45 μm pore size and Isopore membrane filters 5 μm pore size were purchased from EMD Millipore, CA. 1× phosphate buffered saline (PBS) and Quant-iT PicoGreen dsDNA assay kit were obtained from ThermoFisher Scientific, MA. Positive photoresist coated gold–chromium–glass wafers were procured from Telic, CA. SU-8 2002 was purchased from Microchem, MA. QuantiTect Probe RT-PCR kit was acquired from Qiagen, MD. Thermophilic protease (ZyGEM PrepGEM blood kit) was obtained from VWR International, PA. DNA HCV complementary oligomer (5′-TTG GGC GTG CCC CCG C-3′), HCV non-complementary oligomer (5′-GTT GGA GCT GGT GGC GTA G-3′), HCV oligomers with 1 and 2 mismatches (5′-TTG GGC TTG CCC CCG C-3′, 5′-TTG GGA GTG CTC CCG C-3′) and HCV primers (5′-TCT TCA CGC AGA AAG CGT CTA GCC ATG GCG T, 5′-CTC GCA AGC ACC CTA TCA GGC AGT ACC ACA A) were procured from Integrated DNA Technologies, IA and were used as received. Peptide nucleic acid (PNA) universal HCV capture probe (N term-Cys-AEEA-GCG GGG GCA CGC CCA A-C term)[22] was purchased from PNA Bio, CA and was used as received. 1.5 and 4.7 mm poly(methyl methacrylate) (PMMA) were acquired from McMaster-Carr, OH. 250 μm PMMA was obtained from Goodfellow Cambridge, UK. Silicone glue (Dow Corning 3145 RTV Clear) and polydimethylsiloxane (PDMS, Sylgard 184 silicone elastomer kit) were procured from Dow Corning, MI. Vivid plasma separation membrane was purchased from Pall, NY. HelixMark standard silicone tubing was acquired from Freudenberg Medical, CA. Chemically inactivated HCV (NATtrol Human Hepatitis C virus) was obtained from ZeptoMetrix, NY. HCV positive patient serum samples (Cat. No. 0310-0055, Lot-9224, 19 982 516 IU mL^{-1}; Cat. No. 0310-0067, Lot-9, 10 500 000 IU mL^{-1}) were purchased from SeraCare Life Sciences, MA.

Fabrication of electrochemical detector chip

The electrochemical detector chip was fabricated using standard photolithographic processes. Briefly, gold electrodes were patterned on glass wafers. The chip was then passivated with 2 μm thick SU-8 2002 with 10 μm apertures patterned to expose the gold electrodes.

Fabrication of nanostructured microelectrodes (NMEs)

The detector chip was rinsed with acetone, IPA and deionized water (DIH_2O), and dried with nitrogen. Electrodeposition of gold was performed using an Epsilon potentiostat (Bioanalytical Systems, IN) with a 3-electrode setup utilizing a Ag/AgCl reference electrode (Bioanalytical Systems, IN), a Pt counter electrode and gold working electrodes with a patterned aperture. The NMEs were formed by electrodeposition in a solution of 50 mM $HAuCl_4$ and 0.5 M HCl with DC potential amperometry at 0 mV for 100 s. A second electrodeposition in 5 mM $PdCl_2$ and 0.5 M $HClO_4$ was performed using DC potential amperometry at −250 mV for 10 s to provide additional nanostructuring.[23]

Functionalization of NMEs with capture probes

50 μL of an aqueous solution containing 2 μM PNA HCV capture probe and 18 μM MCH was pipetted onto the NMEs on the detector chip and incubated overnight in a dark humidity chamber. The chip was then washed three times for 5 minutes each with 0.1× PBS. The chip was backfilled with 1 mM MCH for an hour and then washed with 0.1× PBS three times.

Electrochemical detection

Electrochemical measurements were performed on an Epsilon potentiostat using a three-electrode configuration with NME working electrodes, gold counter and gold pseudo-reference electrodes. An electrocatalytic solution containing 10 μM $Ru(NH_3)_6Cl_3$ and 4 mM $K_3[Fe(CN)_6]$ in 0.1× PBS was used to generate an electrochemical signal when the chip was scanned from 100 mV to −900 mV using differential pulse voltammetry. A pre-scan was first performed on the chip to obtain the background current in the absence of target (I_0). After hybridization, a second scan was performed to obtain the current after binding of target (I_t).

The percentage change in current was calculated as

$$\% \text{ change in current} = (I_t - I_0)/I_0 \times 100,$$

where I_t is the ruthenium reduction current with target and I_0 is the ruthenium reduction current without target present.

Quantitative PCR (qPCR) measurement of viral recovery

Viral recovery through the Vivid plasma separation membrane using chemically inactivated HCV was performed using

qPCR (7500 Real-Time PCR, Applied Biosystems, CA) with a QuantiTect one-step RT-PCR kit following the kit's instructions. Inactivated HCV was spiked into blood and either filtered through the plasma separation membrane (sample) or centrifuged to remove the supernatant (control). 10 μL of the sample was then diluted to a final concentration of 10% plasma, of which 10 μL was added to the qPCR reaction. Thermal viral lysis[24] was achieved during the PCR process.

Exothermic heat generation and measurement

The exothermic reaction between CaO and water was used to generate heat for exothermic lysis. To determine the temperature produced by this reaction in the liquid sample in a PMMA channel, 0.7 g of CaO was added to a chamber which was then bonded to a 250 μm thick PMMA spacer. The CaO chamber attached with the spacer was bonded with a 1.5 mm thick PMMA layer containing a channel that rests overtop of the heating region. The channel was filled with DIH_2O to mimic the sample that would be heated. Another device with just the CaO chamber and the spacer was used to measure the temperature of the reaction at the surface of the spacer layer. 1 mL DIH_2O was pipetted into the CaO chamber to initiate the exothermic reaction. The heat generated was recorded using an IR camera (RAZ-IR Nano, Sierra Pacific Innovations, NV) and analysed using the Guide IRAnalyser software (Wuhan Guide Infrared, China).

Fluorescent validation of exothermic lysis

Staphylococcus epidermidis was used to validate the exothermic lysis. *S. epidermidis* was cultured overnight in 1.5 mL of TSB. The bacteria were concentrated by centrifugation at 10 000 RPM, washed with 1× PBS three times and resuspended in 1× PBS. The bacteria sample was then split into 50 μL aliquots to test the efficiency of exothermic lysis as compared to a positive control which was lysed thermally and bacteria that were not lysed.

Water was added to the CaO chamber of the exothermic heating device to initialize the exothermic reaction and the bacteria sample was pipetted into the channel on top of the heating region. The sample was allowed to sit on top of the heated CaO chamber for 3 minutes to lyse. Thermal lysis was performed as a positive control at 95 °C for 5 minutes in a thermal cycler (Eppendorf, Germany). After lysing, the samples were centrifuged at 14 000 RPM for 10 minutes. 30 μL of the supernatant was removed and bacterial DNA concentration was measured using the Quant-iT PicoGreen kit with a plate reader (SpectraMax M2, Molecular Devices, CA) at 480 nm excitation and 520 nm emission.

Flow rate measurement

Flow rate measurements were obtained by using dyed water in silicone tubing (inner diameter 0.76 mm) connected to the channel being measured. The flow of the dyed water through the silicone tube was recorded using a camera (Canon, Japan) and displacement was calculated using ImageJ (National Institutes of Health, MD).

Fabrication of integrated viral detection device

The three-component integrated viral detection device was modelled using Fusion 360 (Autodesk, CA).

The sample prep, heating and spacer modules were fabricated in 1.5 mm, 4.7 mm and 250 μm thick PMMA respectively, using computer numerical control (CNC) milling (PCNC 770, Tormach, WI).

The PMMA components were aligned and bonded using a previously described thermal-assisted solvent bonding method.[25] Briefly, anhydrous ethanol was allowed to wick into the bonding interface between the aligned components. The bonding stack was then placed on a hydraulic press (Carver, IN), preheated to 70 °C and pressed for 1 minute at 1000 N. 0.7 g of CaO was loaded into the heating module prior to bonding with the spacer.

The electrochemical detector chip functionalized with the capture probe was inserted into the chip slot of the integrated device and sealed with silicone glue. A piece of 0.5 cm × 1 cm Vivid plasma separation membrane was taped to the inlet of the integrated viral detection device. Silicone tubing was inserted into the outlets of the device and glued in place with silicone glue. The tubing was then connected to two 5 mL syringes to provide negative pressure.

Fluid plugs consisting of 100 μL 0.1× PBS (wash buffer) and 200 μL electrocatalytic solution (scan solution) separated by 50 μL air were pipetted sequentially into the wash/assay reagent storage of the sample prep module. The viscous timing liquid storage of the sample prep module contains 10 μL water (temperature ramping), 120 μL air, 12 μL water (lysis timing), 40 μL air, 85 μL water (hybridization timing), 600 μL air, and 50 μL 50% glycerol (flow termination). 1 mL DIH_2O (heat initiation) was loaded into the water storage chamber of the heating module. A 50 μL solution containing 2 μL thermophilic protease, 10 μL red buffer (ZyGEM PrepGEM blood kit) and 38 μL DIH_2O was added to the plasma filter.

Integrated HCV detection

To generate simulated patient whole blood samples, 50 μL HCV positive patient serum was added to 50 μL whole blood that was pre-processed to remove 50 μL of plasma. The new 100 μL blood sample was added to the plasma filter that had been pre-wetted with the thermophilic protease, which prevents protein coagulation during exothermic lysis. The two syringes were pulled and locked in place to generate the vacuum chambers for flow actuation. The plasma was pulled through the plasma filter into the heating/lysis region. After 3 minutes exothermal viral lysis, the sample travelled to the detector chip and the flow rate was decreased to allow for hybridization between the viral RNA and the capture probe over 20 minutes. Post-hybridization, the flow rate was increased to perform washes. When the electrocatalytic solution flowed

over the detector chip, the flow was terminated (due to 50% glycerol entering the resistance channel) and electrochemical measurements detecting the presence of viral RNA were performed using a potentiostat.

Results and discussion

Device overview

The integrated viral detection device consists of three patterned PMMA layers bonded together (Fig. 1A and B). This device uses passive fluidics to perform viral separation from blood, integrated on-chip viral lysis and the electrochemical detection of viral nucleic acids with minimal steps required of a user. The reagents and chemicals required to lyse and detect the blood-borne HCV were dispensed sequentially using a pipette and stored within the heating and sample prep modules, respectively, prior to use. CaO and water were stored within the heating module. Upon mixing, an exothermic reaction occurred which provided the necessary heat for viral lysis. A thin PMMA spacer was used to physically isolate the heating and sample prep modules while allowing heat transfer to occur. The sample prep module contained preloaded wash buffers, the electrocatalytic solution, and flow rate limiting solutions. Fluid flow in the device was actuated using vacuum chambers and the flow rate was controlled by the viscosity of the rate-limiting fluid passing through the narrow resistance channel, which was located immediately before the outlet of the device.

The assay workflow performed within the device is illustrated in Fig. 1C. A whole blood sample was added to the plasma filter on top of the device inlet. Actuating the fluid flow in the device using vacuum chambers caused the water stored in the heating module to enter the CaO storage chamber and initialize the exothermic reaction. This increased the temperature in the heat/lysis region of the sample prep module. At the same time, the plasma from the whole blood sample passed through the filter and entered the heating/lysis region. The sample remained on top of the heating region to release the viral RNA. The lysed sample then flowed to the detector chip and the target RNA sequence hybridized to the capture probes on the detector electrodes. Wash buffers were used to remove non-specifically bound molecules. The flow was halted when the electrocatalytic solution was on top of the detector chip and electrochemical measurements were performed with a potentiostat.

Fluid actuation and flow rate manipulation

Passive flow actuation in the integrated viral detection device was achieved using vacuum suction (Fig. 2A). A narrow resistance channel with an extremely high flow resistance was used to limit the maximum flow rate in the device to a very consistent and reproducible value (see ESI† for calculations).

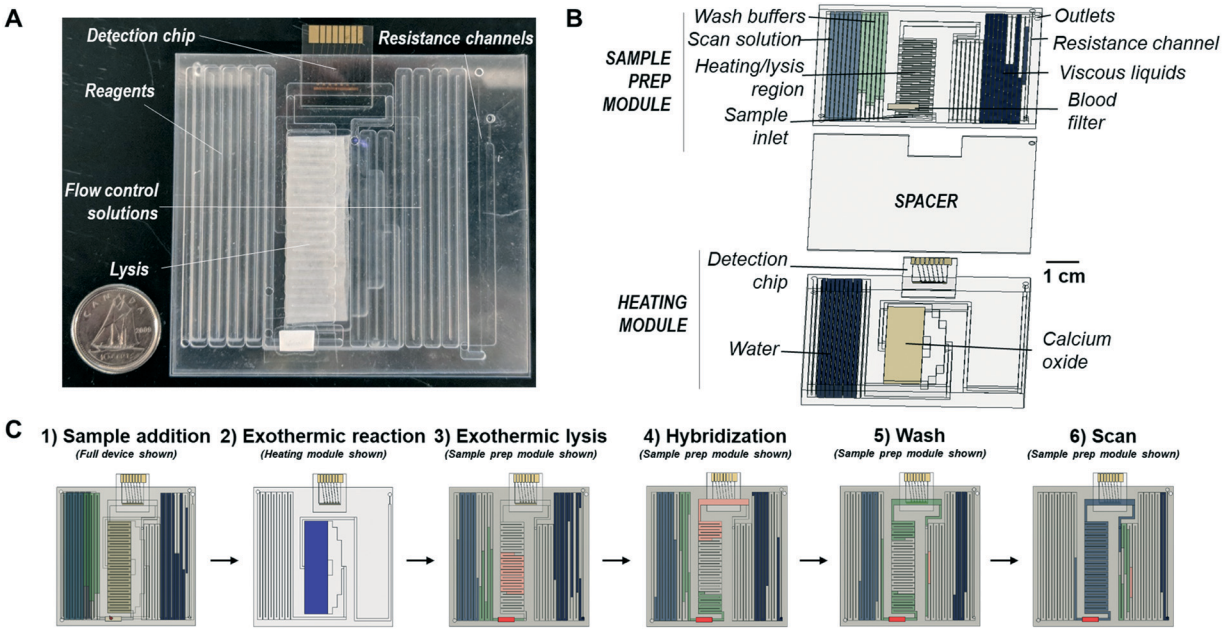

Fig. 1 Device overview. A) Photograph of the integrated viral detection device (dime for scale). B) Schematic of viral detection device consisting of three PMMA layers. The heating module contains storage for CaO and water, which when mixed provide exothermic lysis of the virus. The spacer acts as a physical barrier to prevent mixing of solutions between the heating and sample modules while allowing for heat transfer. The sample module contains preloaded wash buffers and assay reagents. The flow rate is controlled by the viscosity of the fluid flowing through the resistance channel. C) Workflow of detection assay in the viral detection device. 1) Blood is added to integrated device. 2) Water mixes with CaO to start exothermic reaction (heating module). 3) Sample is exothermically lysed (sample prep module). 4) Lysed sample hybridizes to detector chip (sample prep module). 5) Washes remove non-specific binding (sample prep module). 6) Electrochemical measurements performed when scan solution reaches detector chip (sample prep module).

Since flow rate is inversely proportional to flow resistance, the overall flow rate in the device was controlled passively by changing the viscosity of the fluid passing through the flow-limiting resistance channel at any given time (Fig. 2B). When a low viscosity fluid like air passed through the resistance channel, the flow resistance was low and therefore the flow rate was at its maximum. Increasing the flow resistance by passing more viscous fluids, such as water and 50% glycerol, through the resistance channel caused the flow rate to decrease by more than 100 fold. Variations in the maximum/minimum flow rate for the system could also be achieved by changing the channel geometry (Fig. S1†).

This passive flow actuation method allows for reversible variations of flow rate through changes in fluid viscosity and can be used to produce complex flow rate changes desired in an assay (Fig. 2C). A timing fluid sequence consisting of air/water/air positioned behind the resistance channel can be used to create a fast flow rate during sample processing, a slow flow rate during target hybridization, and a fast flow rate during washes. Repeated runs using the same resistance channel show very consistent and reproducible flow rates for more than 25 minutes. The amount of time a desired flow rate is maintained can also be easily adjusted by changing the volume of the timing fluid.

Blood filtration and loading

A commercial Vivid plasma separation membrane was used to separate blood cells from plasma and virus during whole blood sample pre-treatment without manual intervention. This asymmetric polysulfone membrane can very rapidly separate out plasma with minimal lysis of the blood cells. The filter was positioned on top of the sample channel and attached to the device inlet (Fig. 3A). A hemocytometer was used to evaluate the performance of the filter membrane (Fig. 3B and C). The membrane performed extremely well, with filtered undiluted whole blood containing no detectable cells compared to a 10× diluted unfiltered sample. A qPCR measurement to determine the recovery of HCV through the membrane showed negligible loss of virus to the membrane (Fig. 3D).

The hydrophilicity of the plasma filter allowed it to act as a flow regulator, which is critical in enabling the addition of the blood sample to a system that was preloaded with assay reagents (Fig. 3E). Adding liquid to the hydrophilic membrane rapidly formed an airtight seal that prevented air from short circuiting the system (in the case of a dry or hydrophobic membrane there would be a halt in the flow of the preloaded reagents). After the liquid was pulled into the channel, the pores of the membrane exerted sufficient capillary force to retain enough liquid to maintain the seal. The use of the Vivid membrane as a regulator is shown in Fig. 3F. When sample was added to the filter, the preloaded reagent remained stationary (t = 0–40 s) and flow only occurred through the filter. After the sample was depleted from the filter, the flow of the preloaded reagent resumed (t = 80–100 s). The use of several different membranes acting as flow regulators are shown in Fig. S2.†

Exothermic viral lysis

The exothermic reaction between water and CaO is used to generate heat to perform thermal viral lysis in the device. This method is inexpensive and does not require a power source. Water flow into the CaO chamber generated heat that was transferred through the spacer layer to heat the sample flowing in the sample channel above (Fig. 4A).

This exothermic reaction occurred rapidly and the temperature of the water-filled PMMA channel on top of the heating region reached 65 °C in approximately 1 minute and attained a maximum measured temperature of 86 °C (Fig. 4B). The heat generation at the surface of the spacer layer without the water-filled channel present is also shown in Fig. S3.† This elevated temperature allowed for efficient and rapid viral lysis. The efficiency of the exothermic lysis was evaluated using bacteria since it was difficult to concentrate HCV to a detectable level using methods that do not simultaneously cause viral lysis. The Gram-positive bacterium *S. epidermidis*, which

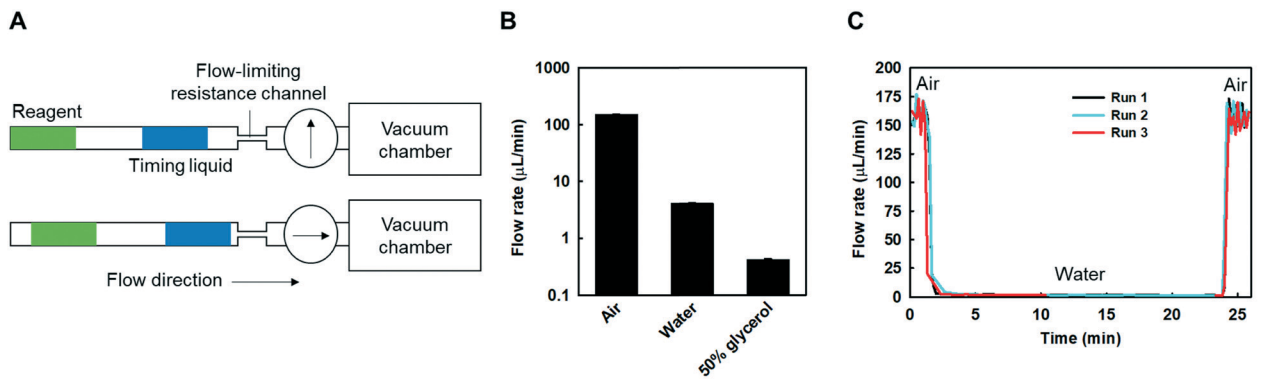

Fig. 2 Passive flow actuation and flow manipulation in the automated device. A) Schematic of flow actuation using a vacuum chamber and a resistance channel that limits the flow rate of the system. The overall flow rate of the system is dictated by the fluid flowing through the resistance channel. B) Flow rate of fluids with various viscosities through a 25 μm × 21 μm × 1 cm resistance channel. C) Reversible changes in flow rate by flowing a sequence of air, water, air through the resistance channel. Error bars represent standard error, n = 5.

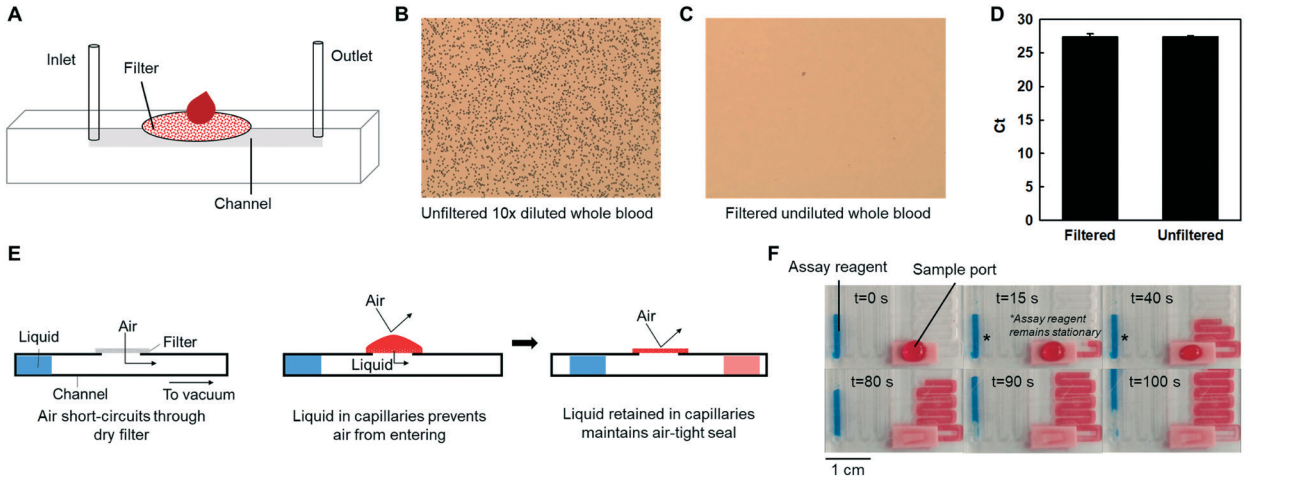

Fig. 3 Properties of blood separation filter membrane. A) Schematic of blood filter system using an asymmetric polysulphone filter. B and C) Hemocytometer image of 10× diluted unfiltered blood (B) *vs.* undiluted blood filtered through the membrane (C). D) Measurement of the recovery of filtered chemically inactivated HCV spiked into blood using qPCR. The recovery is ~99.5%. E) Membrane flow regulator behaviour. Air passing through a dry or hydrophobic membrane will short-circuit the system and prevent the flow of the preloaded liquids. Sample added to a highly hydrophilic membrane forms an air-tight seal and allows the flow of the sample through the membrane. Membranes with strong capillary force can retain sufficient liquid in their pores to maintain the air-tight seal after the sample depletes from the filter. F) Vivid filter membrane acting as a flow regulator. Preloaded assay reagent remains stationary (t = 0–40 s) while flow of the sample occurs through the filter. The flow of the backend reagent resumes when the sample depletes from the membrane (t = 80–100 s). Error bars represent standard error, n = 3.

is more difficult to lyse than HCV due to its strong protective cell wall,[26] was used as a surrogate for validation of exothermic lysis. Using a resistance channel, a 3 minute exothermic lysis was performed on the bacteria. After lysis, the bacterial DNA was detected using PicoGreen dye (Fig. 4C). The fluorescence signal of the lysed sample was approximately 80% of the positive control (lysed at 95 °C for 5 minutes using a thermal cycler).

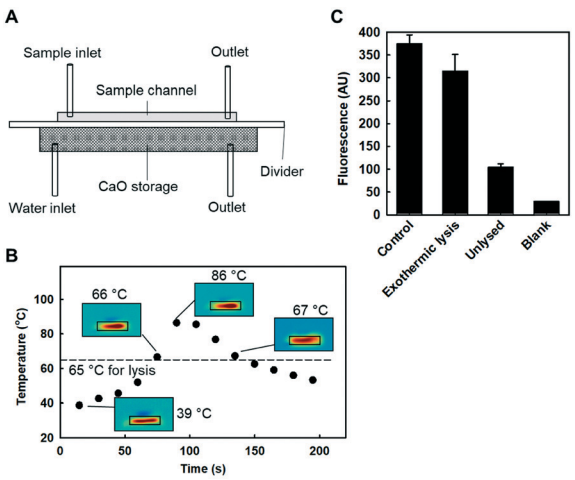

Fig. 4 Integrated exothermic lysis. A) Schematic of prototype exothermic lysis system using the reaction between CaO and water. B) IR measurement of the heat generated by the exothermic reaction as a function of time at the surface of the water-filled PMMA channel on top of the heating region. Dashed line represents 65 °C which is sufficient for the lysis of HCV. Black box represents heating region. C) Validation of exothermic lysis (3 min) through fluorescence detection of gram positive bacteria DNA (*S. epidermidis*). Control lysis is performed in a thermal cycler at 95 °C for 5 min. Error bars represent standard deviation, n = 3.

Detection assay

A label-free charge-based electrochemical assay[23] was used to detect the presence of target HCV RNA (Fig. 5A). Neutral PNA universal HCV capture probes complementary to the conserved 5′ untranslated region of the target HCV RNA were conjugated to the working NMEs on the detector chip. The nanostructuring of the NMEs provides increased surface area for functionalization and enhances sensitivity.[23] An electrocatalytic reporter system comprised of $[Ru(NH_3)_6]^{3+}$ and $[Fe(CN)_6]^{3-}$ was used to readout the presence of target RNA. Hybridizing target RNA to the probe localized negative charges at the surface of the electrode which attracted $[Ru(NH_3)_6]^{3+}$ ions in the electrocatalytic solution. A potentiostat was used to measure the reduction current of $[Ru(NH_3)_6]^{3+}$ converted to $[Ru(NH_3)_6]^{2+}$ when the working electrode was biased at the reduction potential. The reduction current was further amplified by the $[Fe(CN)_6]^{3-}$ ions which regenerated the $[Ru(NH_3)_6]^{3+}$ to allow multiple turnovers.

Initial experiments demonstrated the specificity of the assay by differentiating between complementary and 1 and 2 base pair mismatched DNA oligomers (Fig. S4†). The assay was also used for the analysis of patient HCV in serum prior to on-chip integration (Fig. 5B).

Integrated HCV detection

A schematic of the integrated viral detection device is illustrated in Fig. 5C. The integrated device was prepared as described in the materials and methods section for automated

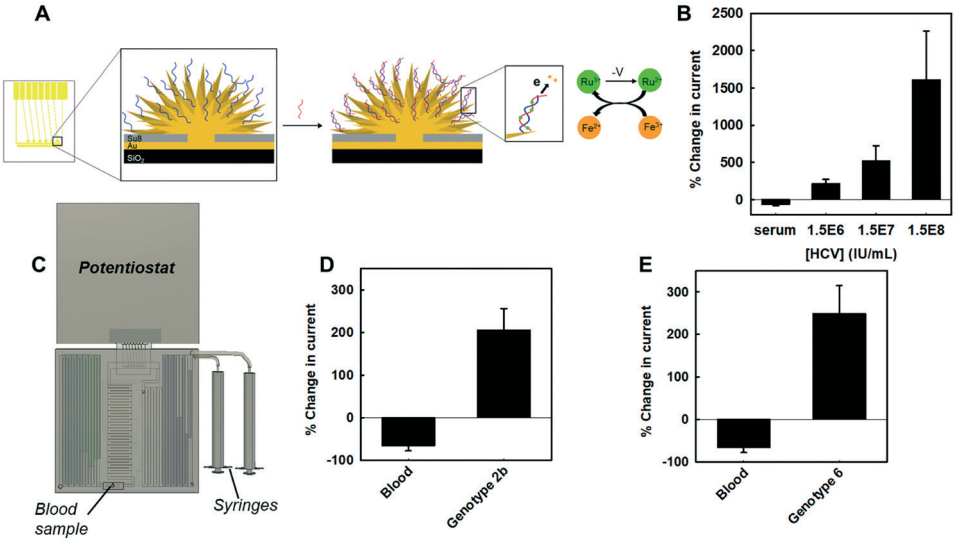

Fig. 5 Detection assay and integrated testing. A) Schematic of electrochemical detection of nucleic acids. Blue strands represent PNA capture probe and red strands represent target RNA. B) Non-integrated electrochemical detection of HCV RNA. C) Schematic of integrated POC viral detection device under operation. Syringes are pulled and locked into place to create vacuum chambers, which actuate fluid flow. A potentiostat is used to perform electrochemical detection of viral nucleic acids. D and E) Detection of HCV positive serum samples spiked into whole blood using the fully integrated device with universal HCV capture probe. Error bars represent standard error, n = 5.

HCV detection. A video of a mock assay run in the integrated device is shown in the ESI.† During the exothermic lysis, a thermophilic protease (derived from *Bacillus* sp. EA1) was activated to degrade the serum proteins to prevent coagulation and assisted with the viral lysis. This thermophilic protease becomes optimally active at 75 °C and can be stably stored between −20 °C to 20 °C.

The integrated viral detection device was used to analyse HCV-positive patient samples of different genotypes in whole blood with a universal HCV capture probe (Fig. 5D and E). The integrated device successfully performed automated sample pre-treatment, a 20 minute target hybridization (Fig. S5†), and electrochemical detection. HCV genotypes 2b and 6 in whole blood were successfully differentiated from HCV-negative whole blood.

The current prototype device does exhibit some variability in the flow rate produced due to the nature of the manufacturing process. The inherent unevenness of the PMMA surface coupled with mechanical micromilling fabrication can cause deviations from the desired height of the resistance channel which influence the flow rate ($Q \propto h^3$). This variability could be significantly reduced by using fabrication methods such as hot embossing and injection moulding that can produce highly reproducible features. Loading of the assay reagents into the device could also be performed with high accuracy using an automated dispensing robot. The redox solution containing both reducing and oxidizing agents could be loaded between nitrogen air gaps for long term storage. The mchip[27] which uses similar plugs of reagents separated by air spacers have shown very good stability of the loaded fluid plugs against shock.[28] Over time, the CaO for the exothermic reaction does absorb moisture from the air. However, this could be mitigated by storing the CaO with desiccant in an on-chip vacuum. The background pre-scan performed in the current prototype can also be obtained using a single electrochemical scan of the detector chip by functionalizing non-complementary probes on some of the electrodes in the final device.

The current integrated device was designed to detect blood-borne viruses in order to showcase its full capabilities to automate the complex sample processing steps required for nucleic acid detection. As such, the device could be used for the detection of other blood-borne viral pathogens, cell-free nucleic acids and pathogenic bacteria in biological fluids with minimum modification.

Conclusion

We report the prototyping of a fully integrated and simple-to-use POC NAT device operated using a passive fluidic method that is capable of detecting viral nucleic acids from blood. The device is able to perform a sequential multi-step assay with modulated flow rates using simple vacuum chambers and minimal user interaction. This inexpensive prototype enabled the detection of patient HCV in blood in approximately 30 minutes. In the future, coupling the device with an inexpensive and portable miniaturized Bluetooth potentiostat (such as the Dstat[29]) to perform the electrochemical detection, and a smartphone to communicate the results could enable rapid diagnosis of blood-borne pathogens at the POC.

Conflicts of interest

There are no conflicts to declare.

Acknowledgements

This work was funded by the Government of Canada through Genome Canada and the Ontario Genomics Institute (OGI-077), the Canadian Institutes of Health Research (148415), the Natural Sciences and Engineering Research Council of Canada (2016-06090), and the Province of Ontario through the Ministry of Research, Innovation and Science (RE-GAPP-6408).

References

1 C. D. Chin, V. Linder and S. K. Sia, *Lab Chip*, 2007, **7**, 41–57.
2 S. O. Kelley, C. A. Mirkin, D. R. Walt, R. F. Ismagilov, M. Toner and E. H. Sargent, *Nat. Nanotechnol.*, 2014, **9**, 969–980.
3 S. Nayak, N. R. Blumenfeld, T. Laksanasopin and S. K. Sia, *Anal. Chem.*, 2017, **89**, 102–123.
4 S. J. Smith, C. R. Nemr and S. O. Kelley, *J. Am. Chem. Soc.*, 2017, **139**, 1020–1028.
5 F. Stumpf, F. Schwemmer, T. Hutzenlaub, D. Baumann, O. Strohmeier, G. Dingemanns, G. Simons, C. Sager, L. Plobner, F. von Stetten, R. Zengerle and D. Mark, *Lab Chip*, 2016, **16**, 199–207.
6 K. Weidemaier, J. Carrino, A. Curry, J. H. Connor and A. Liebmann-Vinson, *Future Virol.*, 2015, **10**, 313–328.
7 N. M. Rodriguez, J. C. Linnes, A. Fan, C. K. Ellenson, N. R. Pollock and C. M. Klapperich, *Anal. Chem.*, 2015, **87**, 7872–7879.
8 L. K. Lafleur, J. D. Bishop, E. K. Heiniger, R. P. Gallagher, M. D. Wheeler, P. Kauffman, X. Zhang, E. C. Kline, J. R. Buser, S. Kumar, S. A. Byrnes, N. M. J. Vermeulen, N. K. Scarr, Y. Belousov, W. Mahoney, B. J. Toley, P. D. Ladd, B. R. Lutz and P. Yager, *Lab Chip*, 2016, **16**, 3777–3787.
9 J. R. Choi, J. Hu, R. Tang, Y. Gong, S. Feng, H. Ren, T. Wen, X. Li, W. A. B. Wan Abas, B. Pingguan-Murphy and F. Xu, *Lab Chip*, 2016, **16**, 611–621.
10 N. M. Rodriguez, W. S. Wong, L. Liu, R. Dewar and C. M. Klapperich, *Lab Chip*, 2016, **16**, 753–763.
11 A. Gansen, A. M. Herrick, I. K. Dimov, L. P. Lee and D. T. Chiu, *Lab Chip*, 2012, **12**, 2247–2254.
12 L. Zhang, Y. Zhang, C. Wang, Q. Feng, F. Fan, G. Zhang, X. Kang, X. Qin, J. Sun, Y. Li and X. Jiang, *Anal. Chem.*, 2014, **86**, 10461–10466.
13 S.-C. Liao, J. Peng, M. G. Mauk, S. Awasthi, J. Song, H. Friedman, H. H. Bau and C. Liu, *Sens. Actuators, B*, 2016, **229**, 232–238.
14 R. Prakash, K. Pabbaraju, S. Wong, R. Tellier and K. V. I. S. Kaler, *Biomed. Microdevices*, 2016, **18**, 44.
15 E.-C. Yeh, C.-C. Fu, L. Hu, R. Thakur, J. Feng and L. P. Lee, *Sci. Adv.*, 2017, **3**, e1501645.
16 Z. Slouka, S. Senapati, S. Shah, R. Lawler, Z. Shi, M. S. Stack and H.-C. Chang, *Talanta*, 2015, **145**, 35–42.
17 R. H. Liu, J. Yang, R. Lenigk, J. Bonanno and P. Grodzinski, *Anal. Chem.*, 2004, **76**, 1824–1831.
18 B. S. Ferguson, S. F. Buchsbaum, J. S. Swensen, K. Hsieh, X. Lou and H. T. Soh, *Anal. Chem.*, 2009, **81**, 6503–6508.
19 B. S. Ferguson, S. F. Buchsbaum, T.-T. Wu, K. Hsieh, Y. Xiao, R. Sun and H. T. Soh, *J. Am. Chem. Soc.*, 2011, **133**, 9129–9135.
20 M. Medina-Sánchez, B. Ibarlucea, N. Pérez, D. D. Karnaushenko, S. M. Weiz, L. Baraban, G. Cuniberti and O. G. Schmidt, *Nano Lett.*, 2016, **16**, 4288–4296.
21 M. Liong, A. N. Hoang, J. Chung, N. Gural, C. B. Ford, C. Min, R. R. Shah, R. Ahmad, M. Fernandez-Suarez, S. M. Fortune, M. Toner, H. Lee and R. Weissleder, *Nat. Commun.*, 2013, **4**, 1752.
22 L. Stuyver, R. Rossau, A. Wyseur, M. Duhamel, B. Vanderborght, H. Van Heuverswyn and G. Maertens, *J. Gen. Virol.*, 1993, **74**, 1093–1102.
23 L. Soleymani, Z. Fang, X. Sun, H. Yang, B. J. Taft, E. H. Sargent and S. O. Kelley, *Angew. Chem., Int. Ed.*, 2009, **48**, 8457–8460.
24 H. Song, J. Li, S. Shi, L. Yan, H. Zhuang and K. Li, *Virol. J.*, 2010, **7**, 40.
25 A. Bamshad, A. Nikfarjam and H. Khaleghi, *J. Micromech. Microeng.*, 2016, **26**, 65017.
26 L. N. Kajiura, S. D. Stewart, J. Dresios and C. F. T. Uyehara, *J. Biomol. Tech.*, 2015, **26**, 118–124.
27 C. D. Chin, T. Laksanasopin, Y. K. Cheung, D. Steinmiller, V. Linder, H. Parsa, J. Wang, H. Moore, R. Rouse, G. Umviligihozo, E. Karita, L. Mwambarangwe, S. L. Braunstein, J. van de Wijgert, R. Sahabo, J. E. Justman, W. El-Sadr and S. K. Sia, *Nat. Med.*, 2011, **17**, 1015–1019.
28 V. Linder, S. K. Sia and G. M. Whitesides, *Anal. Chem.*, 2005, **77**, 64–71.
29 M. D. M. Dryden and A. R. Wheeler, *PLoS One*, 2015, **10**, e0140349.